

Alterations in Tongue Intrinsic Muscles' Fibers Type Following Posterior Teeth Extraction in Albino Rats (An Animal Study)

Original
Article

Lina Ahmed Mohamed Helmy, Mohamed Adel Ahmed, Heba Mohamed Hakam and Israa Ahmed Radwan

Department of Oral Biology, Faculty of Dentistry, Cairo University, Egypt

ABSTRACT

Aim: The aim of the study was to evaluate the effect of posterior teeth extraction on the type of intrinsic muscles' fibers of the tongue.

Methodology: 28 healthy adult male albino rats weight range 150 to 200 gm were randomly divided into 4 groups as following: group I: control 4 weeks, group II: control 8 weeks, group III: bilateral mandibular molars extraction and euthanized after 4 weeks and group IV: bilateral mandibular molars extraction and euthanized after 8 weeks. Tongues were dissected for histological, histomorphometric, gene expression analysis, and ultrastructure examination via transmission electron microscope.

Results: The histological examination of group III showed deterioration in tongue muscles, with areas of spacing between muscle bundles, increased perimysium connective tissue, together with dilated and congested blood. Group IV showed improvement in histological features of muscles together with signs of hypertrophy. Morphometric analysis revealed a significant increase in (mean total area percent of muscle fibers, area of single muscle fiber, perimeter of single muscle fiber and minimum Feret's diameter) in group IV in addition to significant decrease in number of inflammatory cells as compared to group III. Additionally, transmission electron microscopic imaging revealed mitochondrial degeneration together with a statistically significant increase in length of sarcomere and length of I-band in group III. Further a statistically significant increase in width of sarcomere and width of Z-line in addition to increase in Cox IV gene and PGC-1 alpha gene expression was observed in group IV as compared to the other groups.

Conclusions: The current study had shown that bilateral mandibular molar extraction had a great impact on intrinsic muscles of the tongue.

Received: 14 November 2023, **Accepted:** 05 January 2024

Key Words: Cox IV, intrinsic muscles, PCR, PGC-1 alpha, transmission electron microscope.

Corresponding Author: Lina Ahmed Mohamed Helmy, PhD, Department of Oral Biology, Faculty of Dentistry, Cairo University, Egypt, **Tel.:** +20 10 0404 6595, **E-mail:** lina.helmy@dentistry.cu.edu.eg

ISSN: 1110-0559, Vol. 48, No. 1

INTRODUCTION

Tongue is a muscular organ covered with specialized mucosa. Its different muscle groups' unique arrangement and synchronization, allows the tongue to perform its function in speech, deglutition and mastication^[1]. Tongue muscles are classified into extrinsic and intrinsic muscles. The biomechanical system and interaction of both muscles groups is responsible for tongue position, shape, and adaptation^[2]. Intrinsic and extrinsic muscles of the tongue are highly adaptable in response to many inducements, which account for the ability of the tongue to change and adapt its shape and function upon stimulation^[3].

The impact of teeth loss on quality of life and oral cavity health has been widely recognized^[4]. The effects vary with number and location of teeth lost where loss of anterior teeth affects the esthetics mainly while the posterior teeth loss affects the mastication quality^[5].

Teeth loss was suggested to have a deleterious effect on masticatory muscles especially the masseter muscles, reducing the muscle mass and strength^[6]. The thickness of the masseter muscles showed a significant

decrease in edentulous patients as compared to dentate patients. Following a rehabilitation period with dentures in edentulous patients, the masseter muscle showed an increase in thickness which however remained less than the muscle thickness in dentate patients^[7,8].

Cytochrome c oxidase (COX) activity is used to detect changes in tongue intrinsic muscle fibers. COX is the last component of the respiratory chain in mitochondria which has a great role in the regulation of mitochondrial respiration and oxidative phosphorylation^[9]. Because of their higher concentration of mitochondria and oxidative metabolism, type I fibers stain darker when stained with cytochrome c oxidase (COX, complex IV, brown stain). In contrast, type II fibers exhibit a finer and less intensely stained network of mitochondria^[10].

Peroxisome proliferator-activated receptor-gamma coactivator 1 α (PGC-1 α) is a transcriptional coactivator of peroxisome proliferator-activated receptor (PPAR- α) that is responsible of regulating a broad range of processes involved in energy production and consumption. PGC-1 α expression in type I slow fibers is higher than its expression in type II fast fiber^[11,12].

From the forementioned literature, this study was carried out to evaluate the effect of posterior teeth bilateral extraction on tongue's intrinsic muscles' fibers type via histological, histomorphometric, gene expression analysis, and ultrastructure examination via transmission electron microscope (TEM).

MATERIAL AND METHODS

The experiment was held in the animal house, Faculty of medicine, Cairo University after submission for approval from the Institutional Animal Care and Use Committee (IACUC), Cairo University with approval number (CU III F 55 19).

The study was carried out on 28 healthy adult male albino rats weighing from 150 to 200 gm, fed with standard diet pellets and tap water ad libitum. Bilateral mandibular molar extraction was performed on 14 rats, while 14 rats were used as a control group.

Study groups and experiment design

The rats were randomly divided into 4 experimental groups each containing 7 rats. **Group I** (control 4 weeks) and **Group II** (control 8 weeks) were left without teeth extraction as control. **Group III** (Extraction 4 weeks) and **group IV** (Extraction 8 weeks) were subjected to bilateral mandibular molars extraction. Animals were later sacrificed following either 4 weeks (group I and group III) or 8 weeks (group II and group IV).

The experimental unit was tongue of albino rat.

Sample size calculation

As per previous studies^[3,13,14], a total sample size of 28 rats (7 per group) was found adequate to detect an effect size of 0.78, a power of 0.8, a two-sided hypothesis test, and a significance level of 0.05. sample size calculation was done using G*power program, Germany.

Surgical procedures

A 4:1 ketamine/xylazine solution (Amoune Pharmaceutical Co.) was injected intraperitoneally into the animals to induce anesthesia; the dose was 0.15 ml per 100 g of body weight^[15]. The loss of the reflexive blinking of the eyes and the relaxation of the skeletal muscles at the surgical site confirmed the depth and maintenance of anesthesia. The anesthetized animal was placed in supine position to prevent head movement. The operative field was disinfected with alcohol and the extraction site was disinfected with betadine (Providine Iodine 7.5% w/v). All animals in groups III and IV were exposed to the extraction of bilateral mandibular molars under general anesthesia and sterile conditions while group I and group II were anesthetized under the same conditions but without extraction of teeth.

The tongue was held carefully with a mosquito hemostat without injury, the cheeks were retracted using dental mirror. The mandibular molars of rats were extracted atraumatically according to the technique previously

described^[16]. Extraction was done using a curved hemostat with a gentle bucco-lingual movement to perform luxation then extraction. Toothed forceps were used as a root elevator. The root sockets were then inspected, and a small dental curette was used to remove any residual root fragments. Care was taken to remove all blood and debris from the rat's mouth using sterile gauges.

Postoperative care

After surgery, Diclofenac Sodium (Voltaren 75 mg/3ml, Novartis), an analgesic, was administrated intramuscularly to rats from group III (Extraction 4 weeks) and group IV (Extraction 8 weeks) to reduce postoperative edema and pain^[17]. Immediately after surgery, a single dose of 30,000 IU penicillin-G Benzathin was administered to the rats from group III and group IV. All animals were fed a soft diet for a week post-operatively to avoid postsurgical trauma then shifted to a standard diet^[17].

At the end of the experiment, all rats were euthanized either at 4 weeks (group I & group III) or at 8 weeks (group III & group IV) by decapitation. Tongues from 28 rats were dissected for histological, histomorphometric, gene expression analysis, and ultrastructure examination via transmission electron microscope.

The tongue was cut longitudinally into two halves (right and left) the right half was fixed in 10% neutral-buffered formalin for hematoxylin & eosin (H&E) staining and histological examination. The left half was cut into 2 halves where the anterior half was fixed in 3% glutaraldehyde in 0.1 M cacodylate buffer (pH 7.4) for TEM examination while the posterior half was prepared for RNA extraction.

Laboratory procedures

Histological and histomorphometric analysis

For twenty-four hours, the right half of the tongue was embedded in 10% neutral-buffered formalin. After going through a series of graded alcohols and xylene, the samples were embedded in paraffin wax. Sections of 4 microns thickness were fixed on glass slides and stained with H&E^[18]. All specimens were examined using the Leica Qwin 500 (Leica microsystems Inc., Switzerland) light microscope in the Oral Biology department, Faculty of Dentistry, Cairo University, with magnification power 40, 100 and 400. For histological examination, three non-serial sections were examined for each specimen. Histomorphometry analysis of the hematoxylin & eosin-stained sections was performed using the image analysis software Image J (NIH). Five non-overlapping fields for every slide at magnification power of 400 were analyzed for: the total area percent of muscle fibers, area of single muscle, perimeter of single muscle, minimum Feret's diameter, and number of inflammatory cells.

The minimal 'Feret's diameter' parameter is defined as the minimum distance between parallel tangents at opposing borders of the muscle fiber, where it is very insensitive against deviations from the optimal cross-sectioning profile^[19].

Ultrastructure evaluation via transmitting electron microscope and morphometric analysis

The lingual muscle specimen was submerged in a glass specimen vial containing 3% glutaraldehyde. 1% osmium tetroxide was carefully and attentively dispensed into the specimen vial under a chemical fume hood. The osmium tetroxide was removed then the buffering solution was added and finally the resin embedding material is added. Utilizing a Reichert-Jung Ultracut E ultramicrotome, ultrathin sections (70 nm) were cut^[20]. The ultrathin sections were double stained with uranyl acetate and lead citrate. The specimen was examined using a TEM apparatus (Joel Jem 1400, Japan) at the Agriculture Research Centre. TEM images were acquired and were subjected to histomorphometric analysis using image J software to measure the following:

- Sarcomere length: which is the distance between two successive z-lines^[21],
- Sarcomere width: which was measured from the edge of the sarcomere to the opposing end parallel to the M-line^[22],
- I-band length: which is a light zone as it is formed of thin actin filaments and centered by Z-line^[23] which was measured from the border of the light zone to the other border crossing the Z-line^[24].
- H-zone length: which is the light area centered by the M line^[23], it was measured from the border of the light zone to the other border crossing the M-line^[25].
- The Z-lines: it extends from the lateral borders of the sarcomere where the thin filaments are anchored as previously defined^[23]. The width of the Z-line is measured horizontally from its border to the other border^[26], while the length of Z- the line was measured by the vertical line in the center of the Z-line^[27].

Polymerase chain reaction (PCR) for gene expression of Proliferator-activated receptor-gamma coactivator 1 α (PGC1- α) and Cytochrome c oxidase (COX) (complex IV)

It was used to measure the expression of PGC1- α and COX-IV gene in the intrinsic tongue muscles. RNA extraction and cDNA synthesis for PCR were performed in Biochemistry department, Faculty of Medicine, Cairo University.

i. RNA extraction

After homogenizing lingual tissues, total RNA was obtained using a Qiagen tissue extraction kit (Qiagen, USA) in compliance with the manufacturer's instructions. After excising 30 mg of the tissue specimen and chopping it up, Lysis Buffer RLT was utilized to lyse the tissue. and the lysed specimen had been homogenized with a tissue homogenizer for 40 seconds. After centrifuging the lysate

for three minutes at maximum speed, the supernatant was carefully separated and put into a fresh microcentrifuge tube. The cleaned lysate was then mixed with 350 μ l of 70% ethanol. 700 μ l of the material were moved to a RNeasy spin column, which was then put in a 2 ml collecting tube. The sample was centrifuged at 8000 rpm for 15 seconds. To wash the spin column membrane, 700 μ l of Buffer RW1 was added to the RNeasy spin column and centrifuged for 15 seconds at a speed of 8000 rpm.

To wash the spin column membrane, 500 μ l of Buffer RPE was introduced to the RNeasy spin column and centrifuged for 15 seconds at a speed of 8000 rpm. To wash the spin column membrane, 500 μ l of Buffer RPE was introduced to the RNeasy spin column and centrifuged for two minutes at a speed of 8000 rpm. A fresh 1.5 ml collection tube was filled with the RNeasy spin column. To extract the RNA, 30–50 μ l of RNase-free water was directly added to the spin column membrane and centrifuged for 1 minute at 8000 rpm. To be used later, the eluate was moved to a fresh Eppendorf tube and kept cold (-80 °C). Using spectrophotometry (dual wavelength Beckman, Spectrophotometer, USA), the concentration and purity of RNA were determined.

ii. cDNA synthesis

Fermentas, USA, utilized a high-capacity cDNA reverse transcription kit to convert 0.5–2 μ g of total RNA into cDNA. After 5 minutes at 65°C in the heat cycler, 10 μ l of RNA was denatured and 3 μ l of primers were added. At 4°C, the RNA primer mixture was cooled. For every sample, the cDNA master mix was made in accordance with the kit's instructions and added. The master mix of cDNA. For every sample, the master mix had a total volume of 19 microliters. After adding this to the 31 μ l RNA-primer mixture, 50 μ l of cDNA was produced.

After the final mixture was incubated for an hour at 37°C in the programmed thermal cycler, the enzymes were inactivated for ten minutes at 95°C, and then the mixture was cooled. Then RNA was changed into cDNA. The converted cDNA was stored at -20 °C. cDNA was amplified in a minimum of triplicates and a no-template-control (NTC) was included in each reaction. A two-minute denaturation step at 95°C preceded the 35 cycles of amplification, which were 30 seconds at 95°C, 30 seconds at 60–65°C, and 30 seconds at 72°C. Melt curve analysis was used to evaluate the specificity of amplification between 60 and 99°C. For every reaction, the RT-qPCR amplification efficiency (E) was calculated.

The Rotor-Gene 6000 software (version 6) was used to determine the quantification cycle number (Cq) values, which are defined as the number of cycles required to reach a particular fluorescent signal threshold of detection. (12). GAPDH mRNA levels were used as a reference to normalize the samples' average relative gene expression intensity. Primer's sequence specific for each gene as following table (Table 1).

Table 1: The primer sequence of the studied genes

Primer sequence	
PGC1 α	Forward primer :5'-CGGAAATCATATCCAACCAG-3' Reverse primer: 5'-TGAGGACCGCTAGCAAGTTTG-3'
COX-IV	Forward primer :5'-CTATGTGTATGGCCCCATCC-3' Reverse primer: 5'-AGCGGGCTCTCACTTCTTC-3'
GAPDH	Forward primer :5'-ATCGTGGGGCGCCCCAGGCAC-3' Reverse primer: 5'-CTCCTTAATGTCACGCACGATTTC-3'

Statistical Analysis

The numerical data obtained from the histomorphometric analysis for H& E (the area of single muscle, minimum Feret's diameter, perimeter of single muscle, number of inflammatory cells and total area of percent of muscle fibers) , TEM (length of sarcomere, width of sarcomere, length of I-band , length of H-zone, length of z-line and width of z-line) and qRT-PCR (PGC1 α & Cox IV) were analyzed using IBM SPSS advanced statistics (Statistical Package for Social Sciences), version 18 (SPSS Inc., Chicago, IL).

Data were presented as the mean and standard deviation (SD). Since data was normally distributed, a 2 way (ANOVA) statistical method was used to assess the effect of extraction in different time periods. This was followed by Tukey's post hoc test when ANOVA indicated a significant difference. A value of $p < 0.05$ was considered statistically significant.

RESULTS

Histological examination of H&E-stained sections results

Histological examination of the tongue muscles of group I (control 4 weeks) showed normal anatomy and histology of intrinsic tongue muscles where both the cross sectioned transverse muscle and the longitudinal fibers of vertical muscle were well arranged, with normal perimysium connective tissue separating bundles of muscle fibers and displaying normal blood vessels (Figure 1A). Muscle fibers demonstrated homogenous acidophilic sarcoplasm with multiple peripheral flat nuclei below the well-defined sarcolemma, muscle fiber striations were clear in vertical muscle, together with normal perimysium and small blood capillaries (Figure 2A).

Histological examination of the tongue muscles of group II (control 8 weeks) revealed the same normal anatomy and histology as group I. Vertical muscle fibers and transverse muscle fibers were well aligned, with normal perimysium connective tissue surrounding the muscle bundles. Small blood vessels with thin walls were also apparent (Figure 1C). Peripheral nuclei beneath the sarcolemma were noticed in the muscle fibers, muscle fiber striations were apparent in vertical muscles (Figure 2C).

Histological examination of the tongue muscles of group III (extraction 4 weeks) revealed alteration in normal intrinsic muscle histology. Disarrangement of vertical and transverse muscles with muscle bundles haphazardly

arranged. Large spacing between the muscle's bundles of transverse and vertical muscles was distinct (Figure 1B) Inflammatory cells were detected scattered within the perimysium surrounding the muscle bundles and infiltrated between the muscle fibers (Figures 1B,2B). Excessive perimysium tissue separating muscle fibers was detectable. Congested blood vessels with distinct blood corpuscles and blood vessels with thickened lining were also detectable. Additionally, higher magnification revealed obvious distortion of muscle fibers where, some fibers lacked nuclei while other muscle fibers showed enlarged central nuclei (Figure 2E).

Histological examination of the tongue muscles of group IV (extraction 8 weeks) revealed partial improvement in terms of anatomy and histology of intrinsic tongue muscles with significant reduction in space between muscle fibers as compared to group III . Vertical muscles and transverse muscles showed proper alignment. Large, dilated blood vessels were found within the perimysium connective tissue (Figure 1D). Vertical muscle fibers showed some splitting but retained normal striations along them upon higher magnification (Figure 2D). Numerous fat cells were detected in the connective tissue beneath the superficial longitudinal muscle with few scattered inflammatory cells. Vertical muscle fibers displayed an abnormal wavy outline with loss of boundaries and their nuclei gathered in one spot (Figure 2F).

Histomorphometric analysis of H&E-stained light microscope pictures (Table 2)

A statistically significant decrease in mean total area percent of muscles fibers was recorded in group III (extraction 4 weeks) as compared to the group I, group II, and group IV (extraction 8 weeks) ($p < 0.001$) while the difference between group I, group II, and group IV was statistically insignificant (Figure 5). A statistically significant increase in mean area of single muscles fiber, mean perimeter of single muscles fiber and mean minimum Feret's diameter was recorded in group IV (extraction 8 weeks), as compared to group I (control 4 weeks), group II (control 8 weeks) and group III (extraction 4 weeks), while the difference between group I, group II, and group IV was statistically insignificant (Figures 6,7,8).

Regarding the number of inflammatory cells, statistically significant higher mean value was recorded in group III (extraction 4 weeks) as compared to group I (control 4 weeks) and in group III (extraction 4 weeks) as compared to the group IV (extraction 8 weeks). A statistically significant higher mean value was also recorded in group IV (extraction 8 weeks) as compared to group II (control 8 weeks) ($p = 0.006$) (Figure 9).

Transmission electron microscope examination results (TEM)

TEM examination of Group I (control 4 weeks) revealed normal arrangement of myofibrils, running parallel to each other with minute intermyofibrillar space separating them

and filled with sarcoplasm. Sarcomeres were detected between two successive Z- lines (Figure 3A). Upon higher magnification myofibrils revealed uniform arrangement with light bands (I-band) surrounding the Z-line. A faint narrow region, the H band, could be seen in the middle of the sarcomere transected with a dark M-line. A dark line Z-line was detected crossing the light band. Sarcomeres were detected between two successive Z- lines (Figure 4A).

Transmission electron microscope (TEM) of Group II (control 8 weeks) revealed well aligned myofibrils, running parallel to each other with small intermyofibrillar space separating them filled with sarcoplasm (Figure 3C). The myofibrils showed assembly of light bands (I-band) with dark line Z-line found crossing the light band. A pale narrow region, the H band, could be seen in the middle of the sarcomere with a dark M-line centralized in it. Sarcomeres were detected between two successive Z- lines (Figures 3C,4C). Normal mitochondria separating the myofibrils. Several mitochondria ran along the myofibrils (intermyofibrillar mitochondria) (Figures 3C,4C).

Electron microscope examination of the tongue muscles of group III (extraction 4 weeks) revealed an increase in the intermyofibrillar spaces between the myofibrils. The faint H-zone and the dark M-line were less apparent, the Z-lines were narrower together with less apparent light bands as compared to the control groups (Figure 3B). Upon higher magnification, intermyofibrillar mitochondrial vacuolation with decrease in its number was evident (Figures 3B,4B).

Electron microscope examination of the tongue muscles of group IV (8 weeks after bilateral mandibular molars extraction) showed a significant improvement in histological structure of intrinsic muscles. Myofibrils were detected arranged in parallel fashion with minimum intermyofibrillar spaces. The Z-lines appeared thick in comparison to the control groups with defined I-band, H-zone, and M-line (Figures 3D,4D). Myofibrils appeared

to be thicker in width, the mitochondria were normal and presented between the myofibrils but in less number than the control groups (Figure 4D).

Histomorphometric analysis of Transmission electron microscope images (Table 3)

Histomorphometry analysis of Transmission electron microscope images revealed the highest mean value of the length of sarcomere in group III with a statistically significant difference compared to group I, group II, and group IV. Additionally, a statistically significant decrease in the length of the sarcomere was detected in group IV as compared to the control groups II and I (Figure 10).

Regarding the width of sarcomere, the highest mean value was recorded in group IV as compared to in group III and to the control groups I and II (Figure 11).

A significantly higher mean length of I-band value was recorded in group III compared to group IV and the control groups I and II (Figure 12). Regarding the length of H-zone and the length of Z-line, the difference between the groups was statistically insignificant (Figures 13,14). The highest width of Z-line was detected in group IV compared to group III and the control groups I and II (Figure 15).

PGC1 alpha gene expression and Cox IV gene expression (Table 4)

The highest mean PGC1 alpha gene expression was detected in group IV with a statistically significant difference between groups ($p < 0.05$). A statistically significant higher gene expression was recorded in group IV as compared to group III ($p < 0.05$) (Figure 16). The highest mean Cox IV gene expression was detected in group IV with a statistically significant difference between groups ($p < 0.05$). A statistically significant higher gene expression was recorded in group IV compared to the group III ($p < 0.05$) (Figure 17).

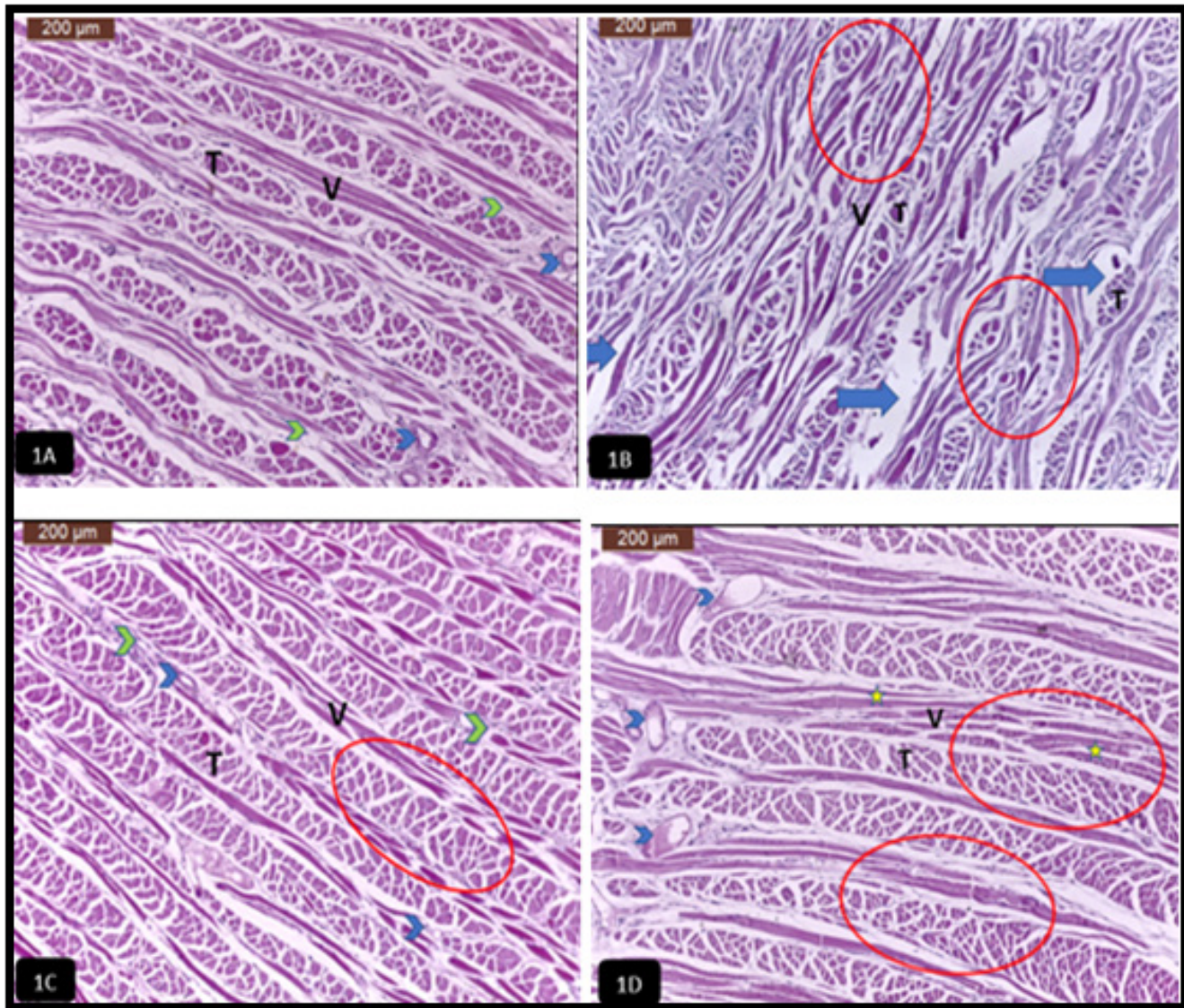


Fig. 1: A photomicrograph of slice in tongue: (A) group I (control 4 weeks) showing normal histological picture of the intrinsic tongue muscles; transverse (T) and vertical (V), normal connective tissue (green arrowhead) with normal blood vessels (blue arrowhead), (B) group III (extraction 4 weeks) showing transverse (T), vertical (V) muscles with haphazardly arranged muscle bundles (red circles), and large spacing between muscle bundles (blue arrow), (C) group II (control 8 weeks) showing normal histological picture of the intrinsic tongue muscles; transverse (T) and vertical (V) muscles, normal arrangement of muscle fibers (circle), normal connective tissue (green arrowhead) with normal blood vessels (blue arrowhead), (D) group IV (extraction 8 weeks) showing the intrinsic tongue muscles, transverse (T), vertical (V) muscles with significant decrease in space between muscle fibers (stars), proper alignment of muscle fibers (circle) and dilated blood vessels (arrowheads) (H&E, Orig. Mag. 100).

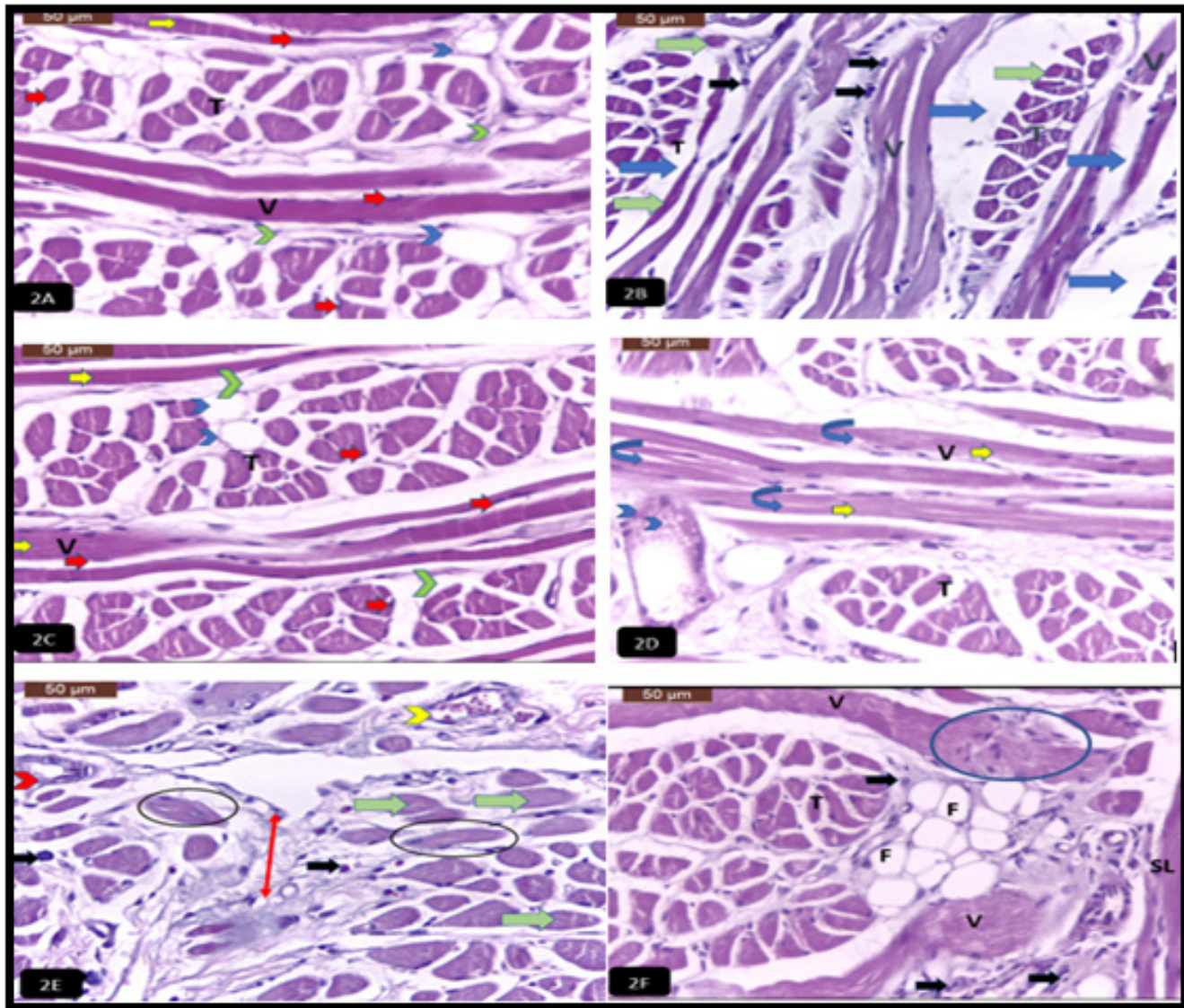


Fig. 2: Photomicrograph of tongue: (A) group I (control 4 weeks) showing the intrinsic tongue muscles; transverse (T) and vertical (V) muscles with normal outline, flat peripheral nuclei beneath sarcolemma (red arrows) and normal perimysium connective tissue (green arrow heads) with small blood capillaries (blue arrow heads) and muscle striations (yellow arrow), (B) group III (extraction 4 weeks) showing transverse (T), vertical (V) muscles some of which lacking nuclei (green arrows), showing normal muscle striations (yellow arrows), large spacing between muscle bundles (blue arrow), and inflammatory cells (black arrow), (C) group II (control 8 weeks) showing transverse (T) and vertical (V) muscles with peripheral flat peripheral nuclei beneath sarcolemma (red arrows), normal connective (green arrowhead) with small blood capillaries (blue arrowhead) and normal muscle striations (yellow arrow) and (D) group IV (extraction 8 weeks) showing transverse (T), vertical (V) muscles, normal muscle striations (yellow arrows) with some fiber splitting (curved arrows) and dilated blood vessel (arrowhead), (E) group III (extraction 4 weeks) showing muscle fiber with large central nuclei (black circle), muscle fibers lacking nuclei (green arrow), inflammatory cells (black arrows), excessive amount of connective tissue (double head arrows), congested blood vessel with red blood corpuscles (yellow arrowhead) and blood vessel with thickening in its wall (red arrowhead), (F) group IV (extraction 8 weeks) showing the intrinsic tongue muscles, superior longitudinal muscles (SL), transverse (T), vertical muscle with abnormal wavy outline (V) with their nuclei gathered at one area (circle), inflammatory cells (black arrows) and fat cells (F) (H&E, Orig. Mag.400).

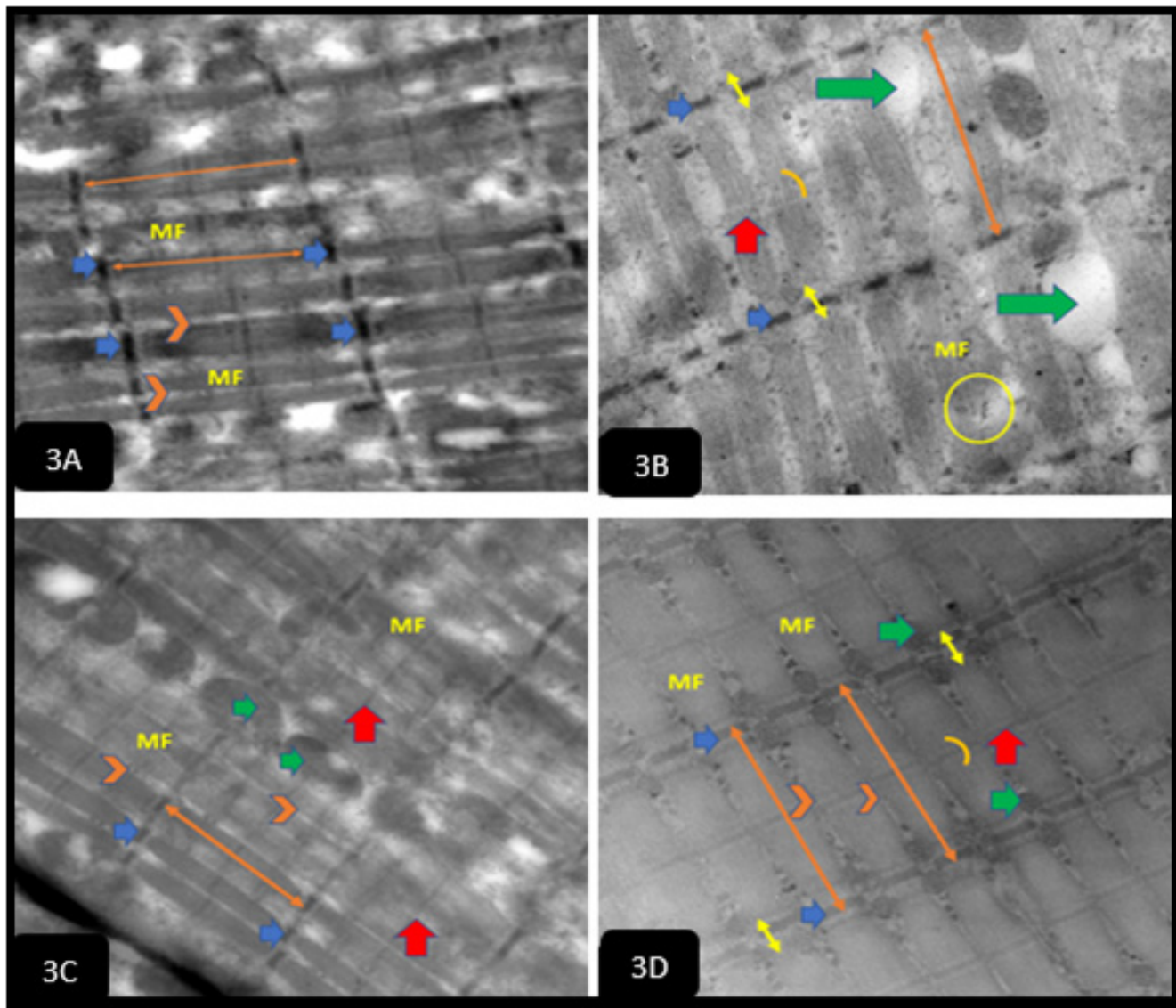


Fig. 3: An electron micrograph of longitudinal section in the tongue: (A) group I (control 4 weeks) showing normal arrangement of parallel myofibrils (MF) with minute intermyofibrillar space (arrowhead), sarcomeres (double head arrow), Z- lines (blue arrows), (B) group III (extraction 4 weeks) showing myofibril (MF) with evident degeneration (circle), sarcomeres (orange double arrow), Z- lines (blue arrows), I-band (yellow double arrow) and intermyofibrillar space (arrowhead), pale H-zone in middle of sarcomere (curved line) transected with M-line (red arrow) and degenerated mitochondria (green arrow), (C) group II (control 8 weeks) showing normal arrangement of parallel myofibrils (MF), sarcomeres (orange double arrow), Z- lines (blue arrows) and intermyofibrillar space (arrowhead), M-line (red arrow) and intermyofibrillar mitochondria (green arrow) and (D) group IV (extraction 8 weeks) showing normal arrangement of parallel myofibrils (MF), sarcomeres (orange double arrow), Z- lines (blue arrows), I-band (yellow double arrow), minimum intermyofibrillar space (arrowhead), pale H- (curved line) transected with M-line (red arrow) and intermyofibrillar mitochondria (green arrow) (TEM, Orig. Mag. 20000).

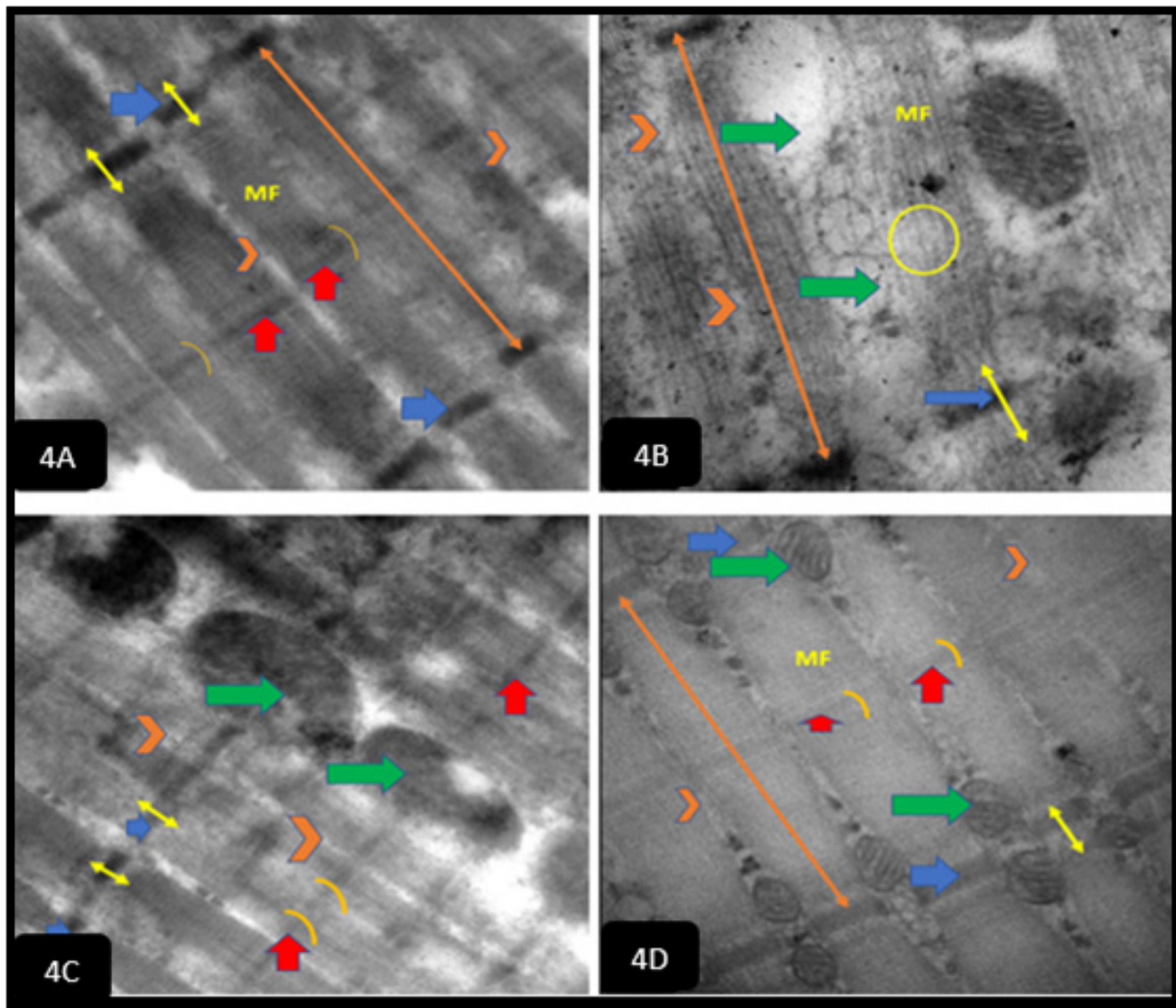


Fig. 4: An electron micrograph of longitudinal section in the tongue: (A) group I (control 4 weeks) a higher magnification showing normal arrangement of parallel myofibrils (MF), sarcomeres (orange double arrow), Z- lines (blue arrows), I-band (yellow double arrow), intermyofibrillar space (arrowhead), pale H-zone (curved line) transected with M-line (red arrow), (B) group III (extraction 4 weeks) showing myofibril (MF) with evident degeneration (circle), sarcomeres (orange double arrow), Z- lines (blue arrows), increase in intermyofibrillar space (arrowhead), I-band (yellow double arrow), intermyofibrillar space (arrowhead), and degenerated mitochondria (green arrow), (C) group II (control 8 weeks) showing normal arrangement of parallel myofibrils (MF), I-band (yellow double arrow) and intermyofibrillar space (arrowhead), pale H-zone (curved line) transected with M-line (red arrow) and intermyofibrillar mitochondria (green arrow), (D) group IV (extraction 8 weeks) showing normal arrangement of parallel thick myofibrils (MF), sarcomeres (orange double arrow), Z- lines that appeared thicker (blue arrows) and I-band (yellow double arrow), minimum intermyofibrillar space (arrowhead), pale H-zone (curved line) transected with M-line (red arrow) and intermyofibrillar mitochondria (green arrow) (TEM, Orig. Mag. 40000).

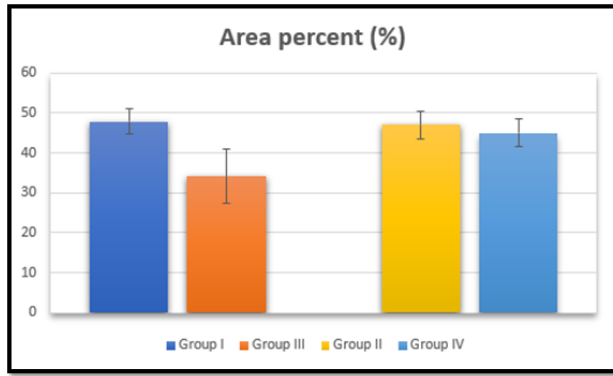


Fig. 5: Bar chart showing mean value of total area % muscle fiber with SD error bars

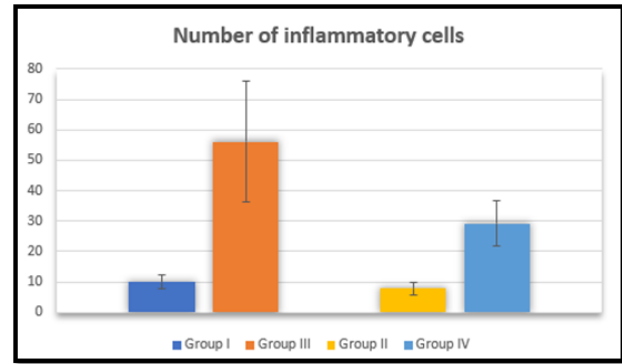


Fig. 9: Bar chart showing mean value of number of inflammatory cells with SD error bars

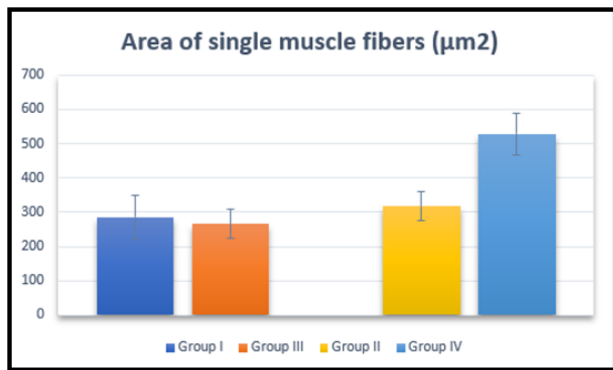


Fig. 6: Bar chart showing mean value of area of single muscle fibers with SD error bars

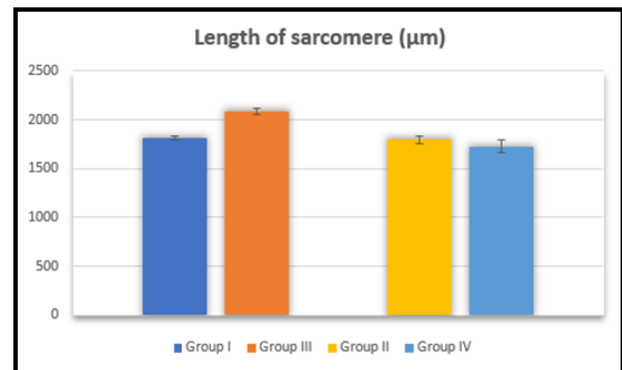


Fig. 10: Bar chart showing mean value of length of sarcomere with SD interval error bars

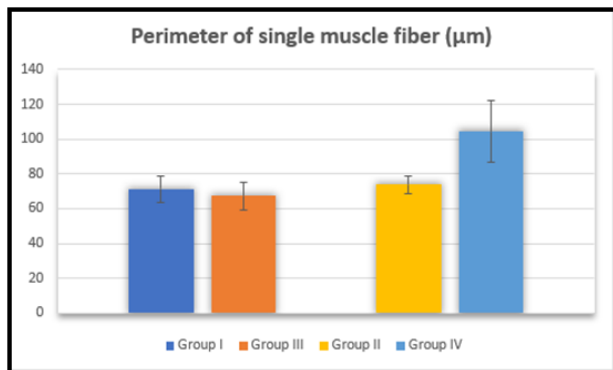


Fig. 7: Bar chart showing mean value perimeter of single muscle fiber with SD error bars

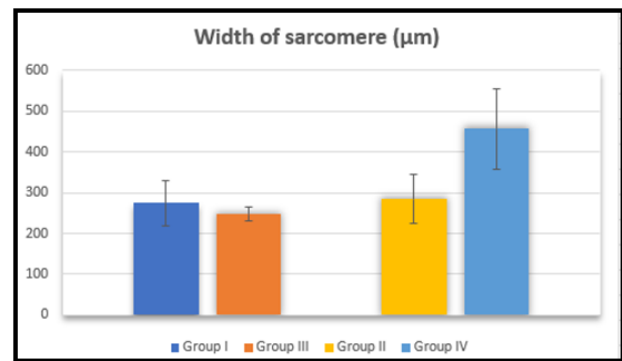


Fig. 11: Bar chart showing mean value of width of sarcomere with SD interval error bars

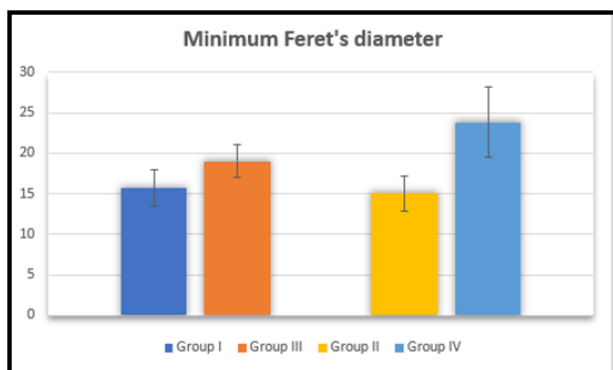


Fig. 8: Bar chart showing mean value of minimum Feret's diameter with SD error bars

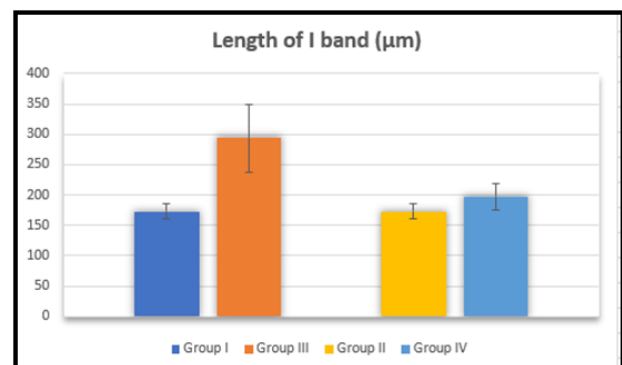


Fig. 12: Bar chart showing mean value of length of I-band with SD error bars

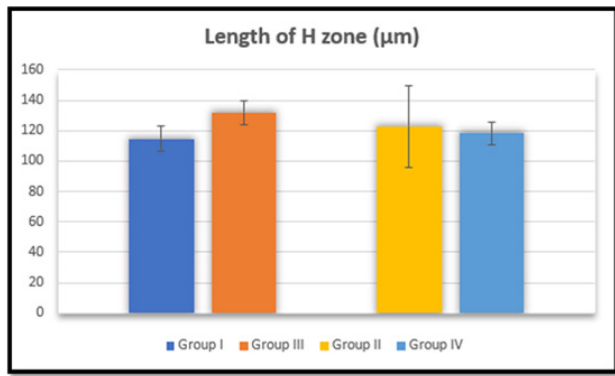


Fig. 13: Bar chart showing mean value of length of H-zone with SD error bars.

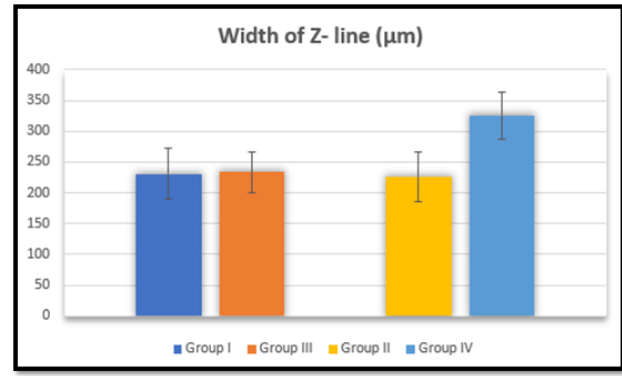


Fig. 15: Bar chart showing mean value of width of Z-line with SD error bars.

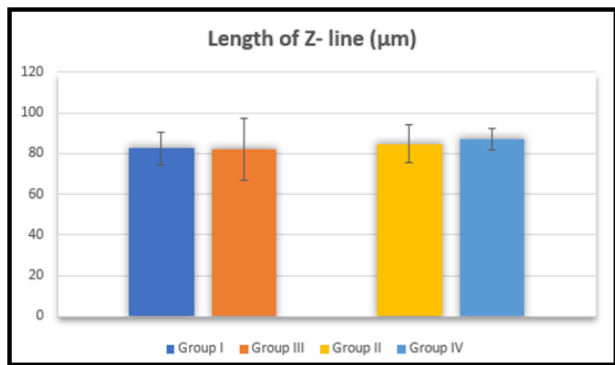


Fig. 14: Bar chart showing mean value of length of Z-line with SD error bars.

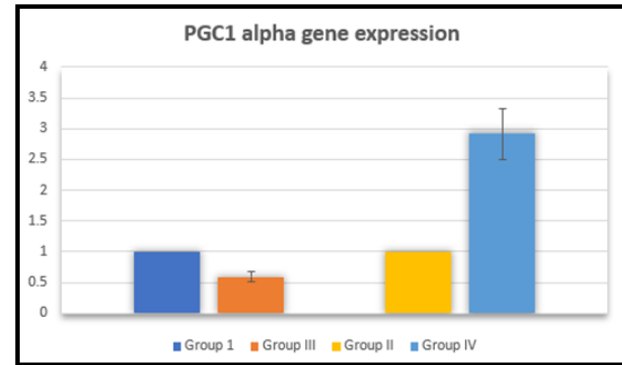


Fig. 16: Bar chart showing mean value of PGC1 alpha gene expression with SD error bars.

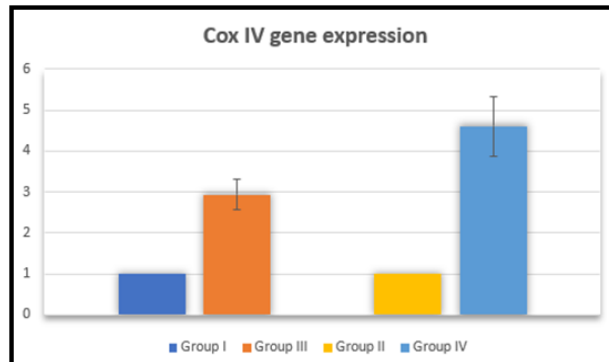


Fig. 17: Bar chart showing mean value of Cox IV gene expression with SD error bars.

Table 2: Descriptive statistics and comparison between groups for LM morphometry; Total area percent of muscles fibers, area of single muscles fibers, perimeter of single muscle fiber, minimum Feret's diameter (Two- ways ANOVA test).

Parameter	Duration	Group	Mean	Std. Error	Min	Max	2 ways ANOVA
							<i>P value</i>
Total area percent of muscles fibers (%)	4 weeks	Group I	47.85±3.23 ^A	1.22	42.05	50.69	0.002*
		Group III	34.14±6.87 ^B	2.60	24.88	41.02	
	8 weeks	Group II	46.97±3.37 ^A	1.28	42.81	50.52	
		Group IV	45.02±3.41 ^A	1.29	40.29	49.47	
Area of single muscles fibers (µm ²)	4 weeks	Group I	286.2±64.4 ^B	24.3	222.6	389.5	0.000*
		Group III	265.7±43.1 ^B	16.3	218.2	356.0	
	8 weeks	Group II	317.8±43.3 ^B	16.4	231.9	360.8	
		Group IV	528.5±60.0 ^A	22.7	427.4	597.2	
Perimeter of single muscle fiber (µm)	4 weeks	Group I	71.22±7.81 ^B	2.95	60.89	82.10	0.000*
		Group III	67.22±8.07 ^B	3.05	57.13	79.77	
	8 weeks	Group II	73.90±5.01 ^B	1.89	68.38	82.72	
		Group IV	104.45±17.90 ^A	6.77	85.34	127.61	
Minimum Feret's diameter (µm)	4 weeks	Group I	15.709±2.273 ^B	0.859	11.488	17.728	0.019*
		Group III	19.037±2.030 ^B	0.767	16.401	22.271	
	8 weeks	Group II	15.019±2.199 ^B	0.831	11.892	17.525	
		Group IV	23.83±4.38 ^A	1.66	19.37	31.91	

Significance level $P < 0.05$, *significant means with different superscript letters are significantly different.

TOOTH LOSS IMPACT ON TONGUE FIBERS FOR

Table 3: Descriptive statistics and comparison between groups for EM morphometry; length of sarcomere (μm), width of sarcomere (μm), length of I band (μm), length of H zone (μm), length of Z line (μm), width of Z (μm) line (Two- ways ANOVA test).

Parameter	Duration	Group	Mean	Std. Error	Min	Max	2 ways ANOVA
							<i>P value</i>
Length of sarcomere (μm)	4 weeks	Group I	1810.6 \pm 20.7 ^B	7.81	1787.9	1849.6	0.000*
		Group III	2081.2 \pm 31.1 ^A	11.8	2050.2	2138.0	
	8 weeks	Group II	1797.9 \pm 42.1 ^B	15.9	1710.9	1839.1	
		Group IV	1729.1 \pm 68.0 ^C	25.7	1609.3	1793.3	
Width of sarcomere (μm)	4 weeks	Group I	274.3 \pm 54.9 ^B	20.8	214.7	360.9	0.000*
		Group III	247.54 \pm 16.47 ^B	6.22	232.74	272.48	
	8 weeks	Group II	283.8 \pm 60.3 ^B	22.8	221.2	373.7	
		Group IV	457.4 \pm 98.7 ^A	37.3	313.7	591.7	
Length of I- band (μm)	4 weeks	Group I	172.71 \pm 12.10 ^B	4.57	158.23	186.51	0.000*
		Group III	293.4 \pm 56.2 ^A	21.3	220.4	364.4	
	8 weeks	Group II	173.28 \pm 11.52 ^B	4.36	157.10	187.62	
		Group IV	197.25 \pm 21.92 ^B	8.29	156.57	225.89	
Length of H -zone (μm)	4 weeks	Group I	114.68 \pm 8.20	3.10	104.38	126.84	0.065
		Group III	132.10 \pm 7.95	3.01	121.45	144.84	
	8 weeks	Group II	122.9 \pm 27.1	10.3	100.3	181.7	
		Group IV	118.20 \pm 7.15	2.70	109.42	129.26	
Length of Z- line (μm)	4 weeks	Group I	82.62 \pm 8.02	3.03	71.65	96.77	0.700
		Group III	82.06 \pm 15.22	5.75	64.87	101.85	
	8 weeks	Group II	84.74 \pm 9.25	3.50	72.48	95.99	
		Group IV	87.16 \pm 5.09	1.92	80.02	93.47	
Width of Z- line (μm)	4 weeks	Group I	231.3 \pm 42.1 ^B	15.9	185.4	294.5	0.003*
		Group III	233.6 \pm 32. ³ ^B	12.2	195.5	280.7	
	8 weeks	Group II	226.5 \pm 40.9 ^B	15.4	182.1	282.7	
		Group IV	325.7 \pm 37.6 ^A	14.2	276.2	373.8	

Significance level $P < 0.05$, *significant

means with different superscript letters are significantly different.

Table 4: Descriptive statistics and comparison between groups for PGC1 alpha gene expression and Cox IV gene expression (Two- ways ANOVA test).

Parameter	Duration	Group	Mean	Std. Error	Min	Max	2 ways ANOVA
							<i>P value</i>
PGC1 alpha gene expression	4 weeks	Group I	1 ^B	0.00	1	1	0.000*
		Group III	0.5884±0.0815 C	0.0308	0.4810	0.6960	
	8 weeks	Group II	1 ^B	0.00	1	1	
		Group IV	2.921±0.416 A	0.157	2.335	3.439	
Cox IV gene expression	4 weeks	Group I	1 ^C	0.00	1	1	0.000*
		Group III	2.939±0.377 B	0.142	2.251	3.377	
	8 weeks	Group II	1 ^C	0.00	1	1	
		Group IV	4.603±0.732 A	0.277	3.440	5.573	

Significance level $P < 0.05$, *significant

means with different superscript letters are significantly different.

DISCUSSION

One of the human body's most flexible and dynamic tissues is the skeletal muscle. The balance between protein synthesis and degradation determines whether muscle mass grows or shrinks, and both processes are influenced by some variables, including dietary status, hormonal balance, physical activity or exercise, injury, and illness^[28,29]. Rats were chosen in the current study due to anatomical similarity between human and rat's tongue muscles^[1,30].

In the ongoing study, group III (extraction 4 weeks) demonstrated dilated congested blood vessels, together with significant increase in inflammatory cells in the perimysium and increased perimysium connective tissue. These findings could be attributed to abnormal mechanical loading on lingual muscles following teeth extraction. Local inflammation of skeletal muscles triggering release of inflammatory cytokines and ROS production induced by intensive and irregular physical activity leading to muscle damage was previously reported^[31,32,33]. Similarly, Teeth extractions in rats were also associated with increased ROS production in medial pterygoid muscle due to altered mechanical loading^[33].

Further, areas of spacing between muscle fibers and muscle bundles observed in group III (extraction 4 weeks), could be attributed to edema subsequent to inflammation and vasodilation of blood vessels together with muscle atrophy and degeneration subsequent to increased mechanical loading. Similar to findings were previously described, where rats strained by eccentric exercise for 2 weeks showed atrophic muscle fibers, inflammatory cells infiltration, spacing between muscle fibers and vasodilatation^[34].

Disarrangement in myofibers of vertical and transverse muscles observed in Group III of the current study can also be attributed to local inflammation due to abnormal forces on lingual muscles. This disarrangement and failure of its

grouping into bundles could be attributed to reduced and disordered muscle fiber subsequent to local inflammation of the muscle^[35].

Myonuclear loss or lack of nuclei in some muscle fibers and central nucleus were also featured in group III (extraction 4 weeks). Myonuclear apoptotic loss could be attributed to increased ROS level due to mitochondrial damage and local inflammation within the muscle^[36]. Muscles fibers with enlarged central nuclei were previously observed where, unilateral anterior crossbite prostheses applied to Sprague-Dawley rats to disrupt the occlusion for two weeks was associated with displacement of muscle fibers' nuclei into a central position instead of peripheral position within masseter and the lateral pterygoid muscles^[37].

The histomorphometric results of group III (extraction 4 weeks) also showed reduction in size of muscle fiber, as demonstrated by significant reduction in mean total area percent of muscle fibers, area of single muscle fiber, muscle fiber perimeter and minimal 'Ferret's diameter' as compared to control groups I & II. This could be attributed to increased oxidative damage, mitochondrial damage^[38] in addition to muscle proteolysis owing to increased inflammatory cytokines and oxidative stress due to mastication function disruption^[39]. These findings augment the histological picture of this group.

The increase in length of sarcomere and I-band observed in group III in the current study is regarded as fast adaptation of muscle fiber to muscle overload specially stretching^[40]. Additionally, thin Z-line was prevalent in group III (extraction 4 weeks). Thin delicate Z-line is a characteristic of fast twitching glycolytic type II fibers and is more prone to damage when the contraction of muscle increases^[41].

On the other hand, group IV (extraction 8 weeks) of the current study, showed decreased spacing between muscle fibers. Our findings coincide with another study that

observed hypertrophy with subsequent decrease in space between muscle fibers in response to muscle damage^[42]. Which implies a regenerative and adaptative process in the muscle of group IV (extraction 8 weeks) of the current study as compared to group III (extraction 4 weeks).

Furthermore, group IV (extraction 8 weeks) showed a statistically significant increase in the mean total area percent of muscle fibers, area of single muscle fiber, perimeter of single muscle fiber and minimum Feret's diameter as compared to group III (extraction 4 weeks) and control groups (group I & II), indicating a significant increase in size of muscle fibers.

Increased total area percent of muscle fibers and area of single muscle fiber in group IV (extraction 8 weeks) can be attributed to increased loading on tongue muscles, owing to teeth loss, leading to hypertrophy of intrinsic tongue muscle. Increased exercise was previously linked to muscle hypertrophy. High resistance exercise induced hypertrophy and increased area of muscle fiber of vastus lateralis muscle of young men^[43]. Similar findings were reported in a study that revealed increased perimeter of single muscle fiber together with its area dictates hypertrophy of the biceps muscle as a result of vertical ladder exercise in albino rats^[44]. Increased minimum Feret's diameter, area of muscle fibers and muscle hypertrophy in association with increased muscular exercise were also demonstrated in a study with a rat model of increased muscle loading of dorsiflexor muscles in the rat hind limb^[45].

It's noteworthy that teeth extraction has a major effect on function of mastication and deglutition. The change in size food particle ingested, restricted growth due to improper nutrient absorption and change in chewing habits in rats after complete removal of molars^[46]. In terms of deglutition, as the number of teeth lost increase the degree of deglutition difficulty increases as the bolus should be grinded to be easily transported by the tongue to the pharynx while the tongue perform anterior sealing together with lips and hard palate^[47,48]. Further, group IV (8 weeks after extraction) showed few inflammatory cells together with increase in size of muscle fiber which coincide with a study that revealed an inverse relationship between the amount of circulating inflammatory cytokines and muscle mass in young men^[49]. Additionally, in the ongoing study, group IV (extraction 8 weeks), also displayed numerous fat cells in the connective tissue beneath the superficial longitudinal muscle together. This could be attributed to chronic inflammation or persistent damage to muscles which can induce adipocytes differentiation from muscle mesenchymal cells^[50].

Fiber splitting in vertical muscles of group IV (extraction 8 weeks) in the current study was revealed. Skeletal muscle fiber branching and splitting is a feature of physiological muscle regeneration following previous damage associated with loading-induced hypertrophy^[51]. Morphological mitochondrial abnormalities are most frequently associated with defects of the respiratory

chain^[52]. Degenerated mitochondria and degeneration in myofibrils were previously attributed to the effect of inflammation associated oxidative stress and ROS production in rats' skeletal muscle^[53,54]. The previous augments finding reported in group III (extraction 4 weeks) of current study as altered mechanical loading was associated with inflammatory and degenerative muscle changes.

Examination of ultrastructure of group IV (extraction 8 weeks) revealed well aligned myofibrils, with minimum intermyofibrillar space. The myofibrils showed assembly of well demarcated light bands (I-band) with dark line Z-line crossing the light band. A pale narrow region, the H band, could be seen in the middle of the sarcomere with a centralized dark M-line. Sarcomeres were detected between two successive Z- lines. Normal mitochondria separating the myofibrils were also observed (intermyofibrillar mitochondria).

Through our current study, increased mechanical loading on tongue muscles, due to teeth loss, was associated with adaptive changes and muscle hypertrophy in group IV (extraction 8 weeks). Similar to our findings, exercise, with subsequent increased mechanical loading, together with anabolic steroids administration in albino rats were associated with quadriceps muscle hypertrophy, normal arrangement of myofibrils and decreased intermyofibrillar spaces at 5 weeks^[55], similar to findings reported in group IV (extraction 8 weeks) of the current study. Previous evidence supports the regenerative and adaptive response of the tongue muscles 8 weeks following teeth extraction. The TEM histomorphometric results of the experimental groups carried out in the present study revealed a statistically significant increase in length of sarcomere, width of sarcomere, length of I-band and width of Z-line of group IV (8 weeks extraction group) as compared to group III (extraction 4 weeks) and control groups.

Further, in the ongoing study, group IV (extraction 8 weeks), showed an increase in the width of sarcomere. Similar finding was described in previous study, where, exercise in mice was associated with increase in the length and width of sarcomere^[56]. Real time quantitative PCR (RT-qPCR) is one of the most important tools nowadays to perform quantitative gene expression^[57]. In the present study Real time quantitative PCR (RT-qPCR) was used to quantify the gene expression level of COX -IV and PGC-1 α in intrinsic lingual muscles. Thick, and strong Z-line is characteristic of slow twitch oxidative type I muscle fiber. This finding coincides with the broad Z-line in group IV (8 weeks extraction group) indicating that the fibers are obtaining characteristics of slow fibers rather than fast type.

COX -IV has been considered as one of the key markers of mitochondrial oxidative capacities in skeletal muscle^[58]. PGC-1 α is a transcriptional co-activator and master regulator of mitochondrial biogenesis^[59] and glucose/fatty acid metabolism^[60]. Multiple stimuli that require

more energy lead to PGC-1 α expression such as exercise due to its role in energy metabolism and mitochondrial biogenesis^[33].

In the present study, statistically significant higher COX -IV gene and PGC-1 α gene expression was observed in group IV (extraction 8 weeks) in comparison to other groups. PGC-1 α significantly increase muscle mitochondrial biogenesis, leading to qualitative changes in muscle fiber from glycolytic to oxidative energy generation^[61]. PGC-1 α expression is a potent marker of slow twitch type I fibers and not fast twitch type II fibers with the ability to shift the type of fiber to type I when highly expressed in the muscle^[11].

Another study demonstrated the significant role of PGC-1 α in conversion of fast glycolytic fibers to slow and oxidative fiber by enhanced mitochondrial respiration and fatty acid oxidation^[62]. In accordance with our results, it was reported increased mitochondrial biogenesis in endurance exercise that was indicated by significant increase of PGC-1 α mRNA expression level in both soleus and gastrocnemius muscle of exercised groups in rats^[63].

Inversely, it was revealed no change in PGC-1 α expression in tongue muscle after exercise^[64]. This finding could support the fact that teeth extraction could have a more deleterious effect on tongue muscles than exercise. Similarly, increased exercise was associated with increased COX -IV expression in rats^[65]. In agreement with our findings, Increase in COX -IV expression together with PGC-1 α expression in gastrocnemius muscles in exercised albino rats for 10 weeks was observed in a previous study^[66].

Judging by the results of the present study, bilateral extraction was associated with parafunctional habits to compensate for teeth loss resulting in increased mechanical loading on the tongue intrinsic muscles associated with inflammation together with ROS production due to mitochondrial damage resulting in degenerative changes in muscles of group III (extraction 4 weeks). It was reported that edentulous and partially dentulous patients often complain of sore tongue due to thrusting against the remaining alveolar ridge and residual teeth^[67,68]. Findings which can be correlated to degenerative changes of the tongue within the current study.

Being a highly adaptive organ, significant improvements in histological picture were detected in muscle tissues of group IV (extraction 8 weeks) of the current study indicating alterations and adaptation in tongue's intrinsic muscles in response to altered mechanical loading. where hypertrophy of muscle fibers, abundance of mitochondria together with large blood vessels were the highlight of histological and ultrastructure examination. Shift to more oxidative and fatigue resistant slow twitch fiber type was ascertained by increased expression of mitochondrial biogenetic marker COX-IV and PGC-1 alpha gene.

CONCLUSIONS

The current study revealed that bilateral mandibular molar extraction had a great impact on intrinsic tongue muscles. We observed that 4 weeks following bilateral extraction of mandibular molars in albino rats was associated with altered mechanical loading on the tongue muscles inducing inflammatory response and muscle atrophy. While 8 weeks post extraction muscle adaptation with hypertrophy took place as evident by histological findings. Additionally, shift in muscle fiber type to slow more fatigue resistant type was clearly evident by elevation of Cox IV gene and PGC-1 alpha gene expression in intrinsic muscles of the tongue. It can be recommended that more studies studying the long-term effects of teeth extraction on various oral and para-oral muscles should be carried out on human patients to fully understand the molecular mechanism behind the muscular changes following teeth loss in edentulous patients.

CONFLICT OF INTERESTS

There are no conflicts of interest.

REFERENCES

1. Sanders, I., & Mu, L. (2013). A three-dimensional atlas of human tongue muscles. *The Anatomical Record*, 296(7), 1102-1114. <https://doi.org/10.1002/ar.22711>
2. Korfage, J. A., Koolstra, J. H., Langenbach, G. E., & Van Eijden, T. M. (2005). Fiber-type composition of the human jaw muscles—(part 1) origin and functional significance of fiber-type diversity. *Journal of Dental Research*, 84(9), 774-783. <https://doi.org/10.1177/154405910508400901>
3. Cullins, M. J., Krekeler, B. N., & Connor, N. P. (2018). Differential impact of tongue exercise on intrinsic lingual muscles. *The Laryngoscope*, 128(10), 2245-2251. <https://doi.org/10.1002/lary.27044>
4. Steele, J. G., Sanders, A. E., Slade, G. D., Allen, P. F., Lahti, S., Nuttall, N., & Spencer, A. J. (2004). How do age and tooth loss affect oral health impacts and quality of life? A study comparing two national samples. *Community dentistry and oral epidemiology*, 32(2), 107-114. <https://doi.org/10.1111/j.0301-5661.2004.00131.x>
5. Gerritsen, A. E., Allen, P. F., Witter, D. J., Bronkhorst, E. M., & Creugers, N. H. (2010). Tooth loss and oral health-related quality of life: a systematic review and meta-analysis. *Health and quality of life outcomes*, 8(1), 126. <https://doi.org/10.1186/1477-7525-8-126>
6. Yamaguchi, K., Tohara, H., Hara, K., Nakane, A., Kajisa, E., Yoshimi, K., & Minakuchi, S. (2018). Relationship of aging, skeletal muscle mass, and tooth loss with masseter muscle thickness. *BMC geriatrics*, 18(1), 67. <https://doi.org/10.1186/s12877-018-0753-z>

7. Bhojar, P. S., Godbole, S. R., Thombare, R. U., & Pakhan, A. J. (2012). Effect of complete edentulism on masseter muscle thickness and changes after complete denture rehabilitation: an ultrasonographic study. *Journal of investigative and clinical dentistry*, 3(1), 45-50. <https://doi.org/10.1111/j.2041-1626.2011.0088.x>
8. Yamaguchi, K., Hara, K., Nakagawa, K., Namiki, C., Ariya, C., Yoshimi, K., Nakane, A., Kubota, K., Furuya, J & Tohara, H. (2020). Association of aging and tooth loss with masseter muscle characteristics: an ultrasonographic study. *Clinical Oral Investigations*, 24, 3881–3888. <https://doi.org/10.1007/s00784-020-03255-y>
9. Capaldi, R. A. (1990). Structure and function of cytochrome c oxidase. *Annual review of biochemistry*, 59(1), 569-596. <https://doi.org/10.1146/annurev.bi.59.070190.003033>
10. Tanji, K., & Bonilla, E. (2008). Light microscopic methods to visualize mitochondria on tissue sections. *Methods*, 46(4), 274-280. <https://doi.org/10.1016/j.ymeth.2008.09.027>
11. Lin, J., Wu, H., Tarr, P. T., Zhang, C. Y., Wu, Z., Boss, O., Michael, L.F., Puigserver, P., Isotani, E., Olson, E.N. & Spiegelman, B. M. (2002). Transcriptional co-activator PGC-1 α drives the formation of slow-twitch muscle fibres. *Nature*, 418(6899), 797-801. <https://doi.org/10.1038/nature00904>
12. Fanelli, M., Filippi, E., Sentinelli, F., Romeo, S., Fallarino, M., Buzzetti, R., Leonetti, F. & Baroni, M. G. (2005). The Gly482Ser missense mutation of the peroxisome proliferator-activated receptor gamma coactivator-1 α (PGC-1 α) gene associates with reduced insulin sensitivity in normal and glucose-intolerant obese subjects. *Disease markers*, 21(4), 175-180. <https://doi.org/10.1155/2005/576748>
13. Shah, F., Stål, P., Li, J., Sessle, B. J., & Avivi-Arber, L. (2019). Tooth extraction and subsequent dental implant placement in Sprague-Dawley rats induce differential changes in anterior digastric myofibre size and myosin heavy chain isoform expression. *Archives of Oral Biology*, 99, 141-149. <https://doi.org/10.1016/j.archoralbio.2019.01.009>
14. Sayed, R. K., de Leonardis, E. C., Guerrero-Martínez, J. A., Rahim, I., Mokhtar, D. M., Saleh, A. M., Abdelmohaimen M. S, Kamal EH A & Acuña-Castroviejo, D. (2016). Identification of morphological markers of sarcopenia at early stage of aging in skeletal muscle of mice. *Experimental gerontology*, 83, 22-30. <https://doi.org/10.1016/j.exger.2016.07.007>
15. Gorustovich, A. A., Steimetz, T., Nielsen, F. H., & Guglielmotti, M. B. (2008). Histomorphometric study of alveolar bone healing in rats fed a boron-deficient diet. *The Anatomical Record: Advances in Integrative Anatomy and Evolutionary Biology: Advances in Integrative Anatomy and Evolutionary Biology*, 291(4), 441-447. <https://doi.org/10.1002/ar.20672>
16. Guglielmotti, M. B., & Cabrini, R. L. (1985). Alveolar wound healing and ridge remodeling after tooth extraction in the rat: a histologic, radiographic, and histometric study. *Journal of oral and maxillofacial surgery*, 43(5), 359-364. [https://doi.org/10.1016/0278-2391\(85\)90257-5](https://doi.org/10.1016/0278-2391(85)90257-5)
17. Mahmoud, E. F., & Hegazy, R. H. (2013). Evaluation of the Role of Bone Marrow-Derived Mesenchymal Stem Cells in Bone Regeneration of Dental Socket in Streptozotocin-Induced Diabetic Albino Rats. *Life Science Journal*, 10(2), 1831-1843.
18. Bancroft, J. D., & Layton, C. (2012). Connective and mesenchymal tissues with their stains. *Bancroft's theory and practice of histological techniques*, 187-214. <https://doi.org/10.1016/B978-0-7020-4226-3.00010-X>
19. Briguet, A., Courdier-Fruh, I., Foster, M., Meier, T., & Magyar, J. P. (2004). Histological parameters for the quantitative assessment of muscular dystrophy in the mdx-mouse. *Neuromuscular disorders*, 14(10), 675-682. <https://doi.org/10.1016/j.nmd.2004.06.008>
20. Thomas, K. C., Zheng, X. F., Garces Suarez, F., Raftery, J. M., Quinlan, K. G., Yang, N., North KN & Houweling, P. J. (2014). Evidence based selection of commonly used RT-qPCR reference genes for the analysis of mouse skeletal muscle. *PloS one*, 9(2), e88653. <https://doi.org/10.1371/journal.pone.0088653>
21. Isola, R., Broccia, F., Casti, A., Loy, F., Isola, M., & Vargiu, R. (2021). STZ-diabetic rat heart maintains developed tension amplitude by increasing sarcomere length and crossbridge density. *Experimental Physiology*, 106(7), 1572-1586. <https://doi.org/10.1113/EP089000>
22. Deng, S., Silimon, R. L., Balakrishnan, M., Bothe, I., Juros, D., Soffar, D. B., & Baylies, M. K. (2021). The actin polymerization factor Diaphanous and the actin severing protein Flightless I collaborate to regulate sarcomere size. *Developmental biology*, 469, 12-25. <https://doi.org/10.1016/j.ydbio.2020.09.014>
23. Ertbjerg, P., & Puolanne, E. (2017). Muscle structure, sarcomere length and influences on meat quality: A review. *Meat science*, 132, 139-152. <https://doi.org/10.1016/j.meatsci.2017.04.261>
24. Cury, D. P., Dias, F. J., Sosthenes, M. C. K., Dos Santos Haemmerle, C. A., Ogawa, K., Da Silva, M. C. P., Mardegan Issa, J.P., Iyomasa, M.M & Watanabe, I. S. (2013). Morphometric, quantitative, and three-dimensional analysis of the heart muscle fibers of old rats: transmission electron microscopy and high-resolution scanning electron microscopy methods. *Microscopy Research and Technique*, 76(2), 184-195. <https://doi.org/10.1002/jemt.22151>

25. Nunes, S. S., Miklas, J. W., Liu, J., Aschar-Sobbi, R., Xiao, Y., Zhang, B., Jiang J, Massé S & Radisic, M. (2013). Biowire: a platform for maturation of human pluripotent stem cell-derived cardiomyocytes. *Nature methods*, 10(8), 781-787. Luther, P. K. (2009). The vertebrate muscle Z-disc: sarcomere anchor for structure and signalling. *Journal of muscle research and cell motility*, 30, 171-185. <https://doi.org/10.1038/nmeth.2524>
26. Deane, C. S., Wilkinson, D. J., Phillips, B. E., Smith, K., Etheridge, T., & Atherton, P. J. (2017). "Nutraceuticals" in relation to human skeletal muscle and exercise. *American Journal of Physiology-Endocrinology and Metabolism*, 312(4), E282-E299. <https://doi.org/10.1152/ajpendo.00230.2016> <https://doi.org/10.1152/ajpendo.00230.2016>
27. Burgoyne, T., Muhamad, F., & Luther, P. K. (2008). Visualization of cardiac muscle thin filaments and measurement of their lengths by electron tomography. *Cardiovascular research*, 77(4), 707-712. <https://doi.org/10.1093/cvr/cvm117>
28. Frontera, W. R., & Ochala, J. (2015). Skeletal muscle: a brief review of structure and function. *Calcified tissue international*, 96, 183-195. <https://doi.org/10.1007/s00223-014-9915-y>
29. Deane, C. S., Wilkinson, D. J., Phillips, B. E., Smith, K., Etheridge, T., & Atherton, P. J. (2017). "Nutraceuticals" in relation to human skeletal muscle and exercise. *American Journal of Physiology-Endocrinology and Metabolism*, 312(4), E282-E299. <https://doi.org/10.1152/ajpendo.00230.2016>
30. Fogarty, M. J., & Sieck, G. C. (2021). Tongue muscle contractile, fatigue, and fiber type properties in rats. *Journal of Applied Physiology*, 131(3), 1043-1055. <https://doi.org/10.1152/jappphysiol.00329.2021>
31. Ibrahim, M. A. A. H., & Elwan, W. M. (2019). Effect of irinotecan on the tongue mucosa of juvenile male albino rat at adulthood. *International Journal of Experimental Pathology*, 100(4), 244-252. <https://doi.org/10.1111/iep.12333>
32. Taherkhani, S., Suzuki, K., & Castell, L. (2020). A short overview of changes in inflammatory cytokines and oxidative stress in response to physical activity and antioxidant supplementation. *Antioxidants*, 9(9), 886. <https://doi.org/10.3390/antiox9090886>
33. Thirupathi, A., & De Souza, C. T. (2017). Multi-regulatory network of ROS: the interconnection of ROS, PGC-1 alpha, and AMPK-SIRT1 during exercise. *Journal of physiology and biochemistry*, 73(4), 487-494. <https://doi.org/10.1007/s13105-017-0576-y>
34. Rizo-Roca, D., Ríos-Kristjánsson, J. G., Núñez-Espinosa, C., Ascensão, A. A., Magalhães, J., Torrella, J. R., Pagés, T. & Viscor, G. (2015). A semiquantitative scoring tool to evaluate eccentric exercise-induced muscle damage in trained rats. *European journal of histochemistry*: 59(4).245-263. <https://doi.org/10.4081%2Ffej.2015.2544>
35. Zhang, J., Lin, C., Song, Y., Zhang, Y., & Chen, J. (2021). Augmented BMP4 signal impairs tongue myogenesis. *Journal of Molecular Histology*, 52(4), 651-659. <https://doi.org/10.1007/s10735-021-09987-9>
36. Calvani, R., Joseph, A. M., Adhietty, P. J., Miccheli, A., Bossola, M., Leeuwenburgh, C., Bernabei, R. & Marzetti, E. (2013). Mitochondrial pathways in sarcopenia of aging and disuse muscle atrophy. *Biological chemistry*, 394(3), 393-414. <https://doi.org/10.1515/hsz-2012-0247>
37. Zhang, H. Y., Yang, H. X., Liu, Q., Xie, M. J., Zhang, J., Liu, X., Liu, X.D., Yu, S.B., Lu, L., Zhang, M & Wang, M. Q. (2020). Injury responses of Sprague-Dawley rat jaw muscles to an experimental unilateral anterior crossbite prosthesis. *Archives of Oral Biology*, 109, 104588. <https://doi.org/10.1016/j.archoralbio.2019.104588>
38. Guigni, B. A., Callahan, D. M., Tourville, T. W., Miller, M. S., Fiske, B., Voigt, T., Korwin-Mihavics, B., Anathy, V., Dittus, K. & Toth, M. J. (2018). Skeletal muscle atrophy and dysfunction in breast cancer patients: role for chemotherapy-derived oxidant stress. *American Journal of Physiology-Cell Physiology*, 315(5), C744-C756. <https://doi.org/10.1152/ajpcell.00002.2018>
39. Leite, M. A., de Mattia, T. M., Kakihata, C. M. M., Bortolini, B. M., de Carli Rodrigues, P. H., Bertolini, G. R. F., Brancalhão, R.M.C., Ribeiro, L.D.F.C., Nassar, C.A. & Nassar, P. O. (2017). Experimental periodontitis in the potentialization of the effects of immobilism in the skeletal striated muscle. *Inflammation*, 40(6), 2000-2011. <https://doi.org/10.1007/s10753-017-0640-3>
40. Jorgenson, K. W., & Hornberger, T. A. (2019). The overlooked role of fiber length in mechanical load-induced growth of skeletal muscle. *Exercise and sport sciences reviews*, 47(4), 258-259. <https://doi.org/10.1249/JES.0000000000000198>
41. Macaluso, F., Isaacs, A. W., & Myburgh, K. H. (2012). Preferential type II muscle fiber damage from plyometric exercise. *Journal of athletic training*, 47(4), 414-420. <https://doi.org/10.4085/1062-6050-47.4.13>
42. Velleman, S. G., & Clark, D. L. (2015). Histopathologic and myogenic gene expression changes associated with wooden breast in broiler breast muscles. *Avian diseases*, 59(3), 410-418. <https://doi.org/10.1637/11097-042015-Reg.1>

43. West, D. W., & Phillips, S. M. (2012). Associations of exercise-induced hormone profiles and gains in strength and hypertrophy in a large cohort after weight training. *European journal of applied physiology*, 112(7), 2693-2702. <https://doi.org/10.1007/s00421-011-2246-z>
44. Neto, J. P., Rocha, L. C., dos Santos Jacob, C., Barbosa, G. K., & Ciena, A. P. (2021). Postsynaptic cleft density changes with combined exercise protocols in an experimental model of muscular hypertrophy. *European Journal of Histochemistry: EJH*, 65(Suppl 1). <https://doi.org/10.4081%2Fejh.2021.3274>
45. Schmoll, M., Unger, E., Sutherland, H., Haller, M., Bijak, M., Lanmüller, H., & Jarvis, J. C. (2018). SpillOver stimulation: A novel hypertrophy model using co-contraction of the plantar-flexors to load the tibial anterior muscle in rats. *PloS one*, 13(11), e0207886. <https://doi.org/10.1371/journal.pone.0207886>
46. Gyimesi, J., & Zelles, T. (1972). Effect of removal of molars on weight increase and food intake in albino rats. *Journal of Dental Research*, 51(4), 897-899. <https://doi.org/10.1177/00220345720510042801>
47. Kennedy, J. G., & Kent, R. D. (1988). Physiological substrates of normal deglutition. *Dysphagia*, 3, 24-37. <https://doi.org/10.1007/BF02406277>
48. Furuta, M., Komiya-Nonaka, M., Akifusa, S., Shimazaki, Y., Adachi, M., Kinoshita, T., Kikutani, T. & Yamashita, Y. (2013). Interrelationship of oral health status, swallowing function, nutritional status, and cognitive ability with activities of daily living in Japanese elderly people receiving home care services due to physical disabilities. *Community dentistry and oral epidemiology*, 41(2), 173-181. <https://doi.org/10.1111/cdoe.12000>
49. Mikkelsen, U. R., Agergaard, J., Couppé, C., Grosset, J. F., Karlsen, A., Magnusson, S. P., Schjerling, P., Kjaer, M. & Mackey, A. L. (2017). Skeletal muscle morphology and regulatory signalling in endurance-trained and sedentary individuals: The influence of ageing. *Experimental gerontology*, 93, 54-67. <https://doi.org/10.1016/j.exger.2017.04.001>
50. Sciorati, C., Clementi, E., Manfredi, A. A., & Rovere-Querini, P. (2015). Fat deposition and accumulation in the damaged and inflamed skeletal muscle: cellular and molecular players. *Cellular and Molecular Life Sciences*, 72(11), 2135-2156. <https://doi.org/10.1007/s00018-015-1857-7>
51. Murach, K. A., Dungan, C. M., Peterson, C. A., & McCarthy, J. J. (2019). Muscle fiber splitting is a physiological response to extreme loading in animals. *Exercise and sport sciences reviews*, 47(2), 108. <https://doi.org/10.1249%2FJES.0000000000000181>
52. Morán, M., Moreno-Lastres, D., Marín-Buera, L., Arenas, J., Martín, M. A., & Ugalde, C. (2012). Mitochondrial respiratory chain dysfunction: implications in neurodegeneration. *Free Radical Biology and Medicine*, 53(3), 595-609. <https://doi.org/10.1016/j.freeradbiomed.2012.05.009>
53. Al-Serwi, R. H., & Ghoneim, F. M. (2015). The impact of vitamin E against acrylamide induced toxicity on skeletal muscles of adult male albino rat tongue: Light and electron microscopic study. *Journal of microscopy and ultrastructure*, 3(3), 137-147. <https://doi.org/10.1016/j.jmau.2015.03.001>
54. Chaanine, A. H. (2019). Morphological stages of mitochondrial vacuolar degeneration in phenylephrine-stressed cardiac myocytes and in animal models and human heart failure. *Medicina*, 55(6), 239. <https://doi.org/10.3390/medicina55060239>
55. Mohamed, H. Z. E., & Mohamed, H. K. (2022). Histological and immunohistochemical studies of the effects of administration of anabolic androgenic steroids alone and in concomitant with training exercise on the adult male rats skeletal muscles. *Egyptian Journal of Histology*, 45(1), 36-49. <https://dx.doi.org/10.21608/ejh.2021.57128.1413>
56. Pallone, G., Palmieri, M., Cariati, I., Bei, R., Masuelli, L., D'arcangelo, G., & Tancredi, V. (2020). Different continuous training modalities result in distinctive effects on muscle structure, plasticity and function. *Biomedical Reports*, 12(5), 267-275. <https://doi.org/10.3892/br.2020.1283>
57. Mehta, A. S., & Singh, A. (2017). Real-time quantitative PCR to demonstrate gene expression in an undergraduate lab. *Drosophila Information Service*, 100,225-230. https://ecommons.udayton.edu/bio_fac_pub/237
58. Sylviana, N., Natalia, C., Goenawan, H., Pratiwi, Y. S., Setiawan, I., & Tarawan, V. M. (2019). Effect of Short-Term Endurance Exercise on COX IV and PGC-1 α mRNA Expression Levels in Rat Skeletal Muscle. *Biomedical and Pharmacology Journal*, 12(3), 1309-1316. <https://dx.doi.org/10.13005/bpj/1759>
59. Wan, Z., Root-McCaig, J., Castellani, L., Kemp, B. E., Steinberg, G. R., & Wright, D. C. (2014). mouse epididymal adipose tissue. *Obesity*, 22(3), 730-738. <https://doi.org/10.1002/oby.20605>
60. Nascimento, G. C., Malzone, B. L., Iyomasa, D. M., Pereira, Y. C., Issa, J. P. M., Leite-Panissi, C. R., Watanabe, I.S., Iyomasa, M.M., Fuentes, R., Del Bel, E.ara & Dias, F. J. (2020). Beneficial effects of benzodiazepine on masticatory muscle dysfunction induced by chronic stress and occlusal instability in an experimental animal study. *Scientific Reports*, 10(1), 1-10. <https://doi.org/10.1038/s41598-020-65524-w>

61. Jäger S, Handschin C, St-Pierre J, Spiegelman BM (2007) AMP-activated protein kinase (AMPK) action in skeletal muscle via direct phosphorylation of PGC-1 α . *Proceeding of National Acad Science U S A* 104:12017–12022. <https://doi.org/10.1073/pnas.0705070104>
62. Arany, Z., Lebrasseur, N., Morris, C., Smith, E., Yang, W., Ma, Y., Chin, S. & Spiegelman, B. M. (2007). The transcriptional coactivator PGC-1 β drives the formation of oxidative type IIX fibers in skeletal muscle. *Cell metabolism*, 5(1), 35-46. <https://doi.org/10.1016/j.cmet.2006.12.003>
63. Zhang, L., Zhou, Y., Wu, W., Hou, L., Chen, H., Zuo, B., Xiong, Y. & Yang, J. (2017). Skeletal muscle-specific overexpression of PGC-1 α induces fiber-type conversion through enhanced mitochondrial respiration and fatty acid oxidation in mice and pigs. *International journal of biological sciences*, 13(9), 1152. <https://doi.org/10.7150%2Fijbs.20132>
64. Krekeler, B. N., Weycker, J. M., & Connor, N. P. (2020). Effects of tongue exercise frequency on tongue muscle biology and swallowing physiology in a rat model. *Dysphagia*, 35(6), 918-934. <https://doi.org/10.1007/s00455-020-10105-2>
65. Hood, D. A. (2001). Invited review: contractile activity-induced mitochondrial biogenesis in skeletal muscle. *Journal of applied physiology*, 90(3), 1137-1157. <https://doi.org/10.1152/jappl.2001.90.3.1137>
66. Strobel, N. A., Peake, J. M., Matsumoto, A. Y. A., Marsh, S. A., Coombes, J. S., & Wadley, G. D. (2011). Antioxidant supplementation reduces skeletal muscle mitochondrial biogenesis. *Medical Science Sports Exercercise*, 43(6), 1017-24. <https://doi.org/10.1249/mss.0b013e318203afa3>
67. Kumar, L. (2014). Biomechanics and clinical implications of complete edentulous state. *Journal of Clinical Gerontology and Geriatrics*, 5(4), 101-104. <https://doi.org/10.1016/j.jcgg.2014.03.001>
68. Şakar, O. (2016). The Effects of Partial Edentulism on the Stomatognathic System and General Health. *Removable Partial Dentures: A Practitioners' Manual*, 9-15. <http://dx.doi.org/10.1016/j.matpr.2021.01.943>

الملخص العربي

التغيرات في نوع النسيج للعضلات الداخلية للسان بعد خلع الأسنان الخلفية في الجرذان البيضاء (دراسة على الحيوان)

لينا أحمد محمد حلمي، محمد عادل أحمد، هبة محمد حكم، إسراء أحمد جمال الدين رضوان

قسم بيولوجيا الفم، كلية طب الأسنان، جامعة القاهرة، مصر

هدف البحث: كان الهدف من هذه الدراسة هو تقييم تأثير خلع الأسنان الخلفية على نوع ألياف العضلات الداخلية للسان. **المواد و الطرق:** تم تقسيم ٢٨ من الجرذان البيضاء البالغة الأصحاء التي تتراوح وزنها بين ١٥٠ إلى ٢٠٠ غرام عشوائياً إلى أربعة مجموعات كما الآتي: المجموعة الأولى: الضابطة ٤ أسابيع، المجموعة الثانية: الضابطة ٨ أسابيع، المجموعة الثالثة: خلع أضراس الفك السفلي والموت الرحيم بعد ٤ أسابيع والمجموعة الرابعة: خلع أضراس الفك السفلي والموت الرحيم بعد ٨ أسابيع. تم تشريح الأسنان للتحليل النسيجي و التحليل المورفومتري وتحليل التعبير الجيني وفحص البنية التحتية عبر المجهر الإلكتروني النافذ.

النتائج: أظهر الفحص النسيجي للمجموعة الثالثة تدهوراً في عضلات اللسان مع مناطق تباعد بين الحزم العضلية وزيادة في النسيج الضام المحيط بالعضل بالإضافة إلى توسع واحتقان الأوعية الدموية. المجموعة الرابعة أظهرت تحسناً في المظاهر النسيجية للعضلات مع تضخم الألياف. أظهر التحليل المورفومتري زيادة في (متوسط المساحة الكلية للألياف العضلية، مساحة الليف العضلي المفرد، محيط الليف العضلي المفرد والحد الأدنى لقطر الفيريت) في المجموعة الرابعة بالإضافة إلى انخفاض كبير في عدد الخلايا الالتهابية مقارنة بالمجموعة الثالثة. بالإضافة إلى ذلك، كشف التصوير المجهر الإلكتروني النافذ عن تحلل الميتوكوندريا مع زيادة ذات دلالة إحصائية في طول القسم العضلي وطول المنطقة الفاتحة I في المجموعة الثالثة مع كشف زيادة ذات دلالة إحصائية في عرض القسم العضلي وسمك الخطوط Z بالإضافة إلى أعلى تعبير جيني ل Cox-IV و PGC1- α في المجموعة الرابعة. **الاستنتاجات:** كشفت الدراسة الحالية أن خلع جميع الأضراس علي الجانبين في الفك السفلي كان له تأثير كبير على عضلات اللسان.